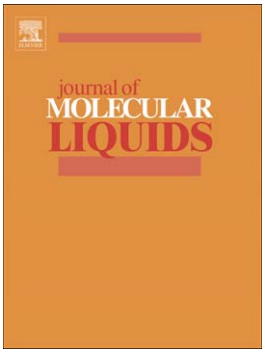

Rheology of Micropolar Fluid in a Channel with Changing Walls: Investigation of Multiple Solutions

Jawad Raza, Azizah Mohd Rohni, Zurni Omar

PII: S0167-7322(16)30928-X
DOI: doi: 10.1016/j.molliq.2016.07.102
Reference: MOLLIQ 6116

To appear in: *Journal of Molecular Liquids*

Received date: 17 April 2016
Accepted date: 22 July 2016

Please cite this article as: Jawad Raza, Azizah Mohd Rohni, Zurni Omar, Rheology of Micropolar Fluid in a Channel with Changing Walls: Investigation of Multiple Solutions, *Journal of Molecular Liquids* (2016), doi: 10.1016/j.molliq.2016.07.102

Rheology of Micropolar Fluid in a Channel with Changing Walls: Investigation of Multiple Solutions

Jawad Raza[a], Azizah Mohd Rohni[a] and Zurni Omar[a]

[a]School of Quantitative Sciences, Universiti Utara Malaysia, 06010 Sintok, Kedah Malaysia

Abstract: A numerical study is carried out in order to investigate the multiple solutions of micropolar fluid in a channel with changing walls. Mathematical modeling of laws of conservation of mass, momentum, angular momentum and energy is performed and governing partial differential equations are converted into self-similar ordinary differential equations by applying suitable similarity transformation and then solved numerically by shooting method. A new branch of solutions is found and presented in graphically and numerically for the various values of parameters, which has never been reported.

Keywords: Micropolar fluid; micro-rotation; multiple solutions; shooting method

1. INTRODUCTION

Based on the solutions of nonlinear problems it can be argued that numerous nonlinear fluid flow problems have multiple solutions. Without a doubt, it is stated that it is very hard to find all the branches of multiple solutions of a given nonlinear fluid flow problem. At the point when two various solutions are close to each other, most of the numerical techniques fail to identify the multiple solutions due to the fact that numerical solution might oscillate between two solutions. Prime objective of the present study is to investigate the multiple solutions of the problem of micropolar fluid in a channel with changing walls (Expanding or Contracting walls).

Chemical engineering, biomedical, science and environmental engineering vigorously adopt fluid flow behavior in a channel particularly the fluids in which shear stresses and rate of change of deformation has nonlinear effect on one another [1-5]. Micropolar fluid is one of the most prominent among them. These fluids actually belong to the following class of fluids having non-symmetrical stress tensor with microstructure molecular bounding. The theory of Micropolar fluid was presented by Eringen [6] in 1953. Complex fluid problems can be studied with the help of Eringen's theory, including flow of blood, liquid crystals, low concentration suspensions & turbulent sheer flows. As compared to the classical Newtonian fluids, Micropolar fluids possess 5 additional coefficients of viscosity. He claimed that the effect of micro-rotations in micro structure model happens in Micropolar fluid. These fluids can support stress momentum and body momentum; are usually influenced by the spin inertia dynamically. As micropolar fluid consists of micro-structures so the effects seen on microscopic level are present on the micro-structure level by the micro motions of fluid elements. Physically they may be explained as the rigid, spherical or bar like elements that are randomly oriented dispersed in a viscous medium and thus the deformation of fluid particles in it are ignored completely. These include fluids having crystals of dumb-bell shaped molecules, like in animal blood. In addition, the mathematical models of the fluids with certain additives or polymeric fluids resembles like the mathematical model of Micropolar fluids [7-15].

Recently, analytical investigation of the problem of micropolar fluid in a porous channel with suction/injection has been made by Aski et al. [16]. Approximate solution of micropolar fluid in a channel subject to heat transfer and chemical reaction was presented by Sheikholeslami et al.

[17]. Homotopy perturbation method (HPM) was used in order to find approximate solution of governing nonlinear differential equations of micropolar fluid. Sajid et al. [18] analyzed the boundary layer flow of a micropolar fluid in a porous channel. Fakour et al. [19] considered the heat transfer analysis on micropolar fluid in a channel analytically and numerically. Approximate solution was obtained by least square method (LSM) and compared the results with Runge–Kutta fourth-order. The study revealed that boundary layer thickness of velocity decrease by increasing the values of Reynold number R. Moreover, fluid temperature increases with the increase in the strength of Peclet number Pe. Hydromagnetic flow of a micropolar fluid between parallel plates with heat transfer was examined by Mehmood et al. [20]. Resulting coupled nonlinear governing equations were solved by optimal homotopy analysis method (OHAM). The study revealed that coupling parameter increases the vortex viscosity of the fluid which reduces the fluid velocity.

2. MATHEMATICAL FORMULATION

Let us consider unsteady, laminar and incompressible micropolar fluid in a channel. Both the channel walls are considered equally permeable and can be expand or contract uniformly with time dependent rate $\dot{a}$. For the uniform wall suction/injection we assume that fluid is symmetric about $y - axis$ to the channel walls as described in physical model Figure 1.

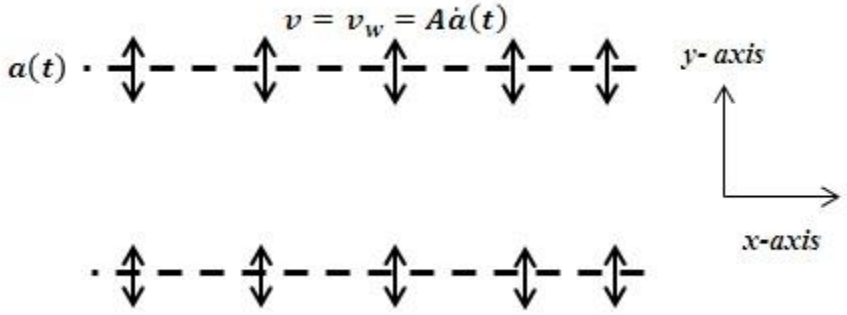

Figure 1: Physical model of the proposed problem

The general equations governing the motion of micropolar fluids as given by Eringen [6] may be expressed as:

$$\frac{\partial \rho}{\partial t} + \nabla \cdot (\rho \bar{V}) = 0 \tag{1}$$

$$(\lambda + 2\mu + \kappa)\nabla(\nabla \cdot \bar{V}) - (\mu + \kappa)\nabla \times \nabla \times \bar{V} + \kappa \nabla \times \bar{v} - \nabla \mathrm{p} + \rho \bar{f} = \rho \dot{\bar{V}} \tag{2}$$

$$(\alpha + \beta + \gamma)\nabla(\nabla \cdot \bar{v}) - \gamma(\nabla \times \nabla \times \bar{v}) + \kappa \nabla \times \bar{V} - 2\kappa \bar{v} + \rho \bar{l} = \rho j \dot{\bar{v}} \tag{3}$$

In these equations (1)-(3), $\bar{V}$ is the velocity field, $\bar{v}$ is the microrotation vector, ρ is the density, p is the pressure, $\bar{f}$ and $\bar{l}$ are the body force and body couple per unit mass respectively, j is the micro-inertia, $\lambda, \mu, \alpha, \beta, \gamma$ and κ are the micropolar material constants (or viscous coefficients), dot signifies material derivatives.

Components of the velocity vector $\bar{V}$ and micro-rotation $\bar{v}$ are in the form of

$\bar{V} = (u(x,y), v(x,y), 0) \qquad \bar{v} = \big(0,0, g(x,y)\big)$

Where, g is the component of the micro-rotation normal to the xy-plane.

Governing equations of the flow for the proposed problem are

$$\frac{\partial u}{\partial x} + \frac{\partial v}{\partial y} = 0 \tag{4}$$

$$u\frac{\partial u}{\partial x}+v\frac{\partial u}{\partial y}=\frac{-1}{\rho}\frac{\partial p}{\partial x}+\frac{\mu+\kappa}{\rho}\nabla^2 u+\frac{\kappa}{\rho}\frac{\partial g}{\partial y} \quad (5)$$

$$u\frac{\partial v}{\partial x}+v\frac{\partial v}{\partial y}=\frac{-1}{\rho}\frac{\partial p}{\partial y}+\frac{\mu+\kappa}{\rho}\nabla^2 v-\frac{\kappa}{\rho}\frac{\partial g}{\partial x} \quad (6)$$

$$\rho\bar{J}\left(u\frac{\partial g}{\partial x}+v\frac{\partial g}{\partial y}\right)=\gamma\nabla^2 g+\kappa\left(\frac{\partial v}{\partial x}-\frac{\partial u}{\partial y}\right)-2\kappa g \quad (7)$$

Suitable boundary conditions for the proposed problem are:

$$\bar{u}(x,a)=0,\quad \bar{v}(a)=-v_w=-A\dot{a}, \quad (8)$$

$$\frac{\partial\bar{u}}{\partial y}(x,0)=0,\ \bar{v}(0)=0 \quad (9)$$

At the channel wall, it is assumed that fluid can be extracted or injected with the constant velocity v_w. Moreover, the coefficient of suction/injection $A\cong {}^{v_w}/_{\dot{a}}$ is a wall permeability parameter appears in Equation (8).

We can develop similar solution in the light of boundary conditions (8)-(9). For this consider $y\equiv\frac{\bar{y}}{a}$ and stream function can be written as;

$$\psi=\frac{\upsilon}{a(t)}\bar{x}\bar{F}(\eta,t),\ g=\nu a^{-3}xG(\eta,t) \text{ where } \eta={}^{y}/_{a(t)} \quad (10)$$

Put it in Equations (4)-(7), we get:

$$(1+C_1)F_{\eta\eta\eta\eta}-C_1G_{\eta\eta}+3\alpha F_{\eta\eta}+\alpha\eta F_{\eta\eta\eta}+\left(F_\eta F_{\eta\eta}-FF_{\eta\eta\eta}\right)-\nu^{-1}a^2F_{\eta\eta t}=0, \quad (11)$$

$$\left(1+\frac{C_1}{2}\right)G_{\eta\eta}+N\alpha\left(3G+\eta G_\eta\right)+NF_\eta G-NFG_\eta-C_1\left(2G-F_{\eta\eta}\right)-\nu^{-1}a^2G_t=0 \quad (12)$$

Where $\alpha=\frac{a\dot{a}}{\nu}$is the wall expansion ratio, $C_1$is vortex viscosity parameter, N is micro-inertia spin parameter. $\alpha>0$ is for expansion and $\alpha<0$ is for contraction.

Here $R=\frac{av_w}{\upsilon}$ is the cross flow Reynolds number and $R>0$ is for injection and $R<0$ for suction through the walls.

For self-similar solution, we consider $f=\frac{\bar{F}}{R}$ and $g=\frac{G}{R}$ by the transformation introduced by Uchida and Aoki [21], Dauenhauer and Majdalani [22]. This can leads us to consider the case α is a constant and $f=f(\eta)$. Therefore, $f_{\eta\eta t}=0$.

In the light of above provisions, Equations (11) and (12) becomes:

$$(1+C_1)f''''-C_1g''+3\alpha f''+\alpha\eta f'''+R(f'f''-ff''')=0, \quad (13)$$

$$\left(1+\frac{C_1}{2}\right)g''+N\alpha(3g+\eta g')+NR(f'g-fg')-C_1(2g-f'')=0 \quad (14)$$

Appropriate boundary conditions are:

$$f'(1)=0, f(1)=1, g(1)=0 \quad (15)$$

$$f(0)=f''(0)=g(0)=0 \quad (16)$$

3. HEAT TRANSFER

For the temperature distribution in the flow field, the governing energy equation can be written as:

$$\frac{\partial T}{\partial t}+\rho C_p\left(u\frac{\partial T}{\partial x}+v\frac{\partial T}{\partial y}\right)=k_\circ\left(\frac{\partial^2 T}{\partial x^2}+\frac{\partial^2 T}{\partial y^2}\right) \quad (17)$$

Here, T is the temperature, $k_\circ$is the thermal conductivity and C_P is the specific heat.

The appropriate boundary conditions are:

$$T=T_H \qquad \text{at } y=a \quad (18)$$

$$T=T_w \qquad \text{at } y=0 \quad (19)$$

Further, the dimensionless temperature θ is introduced as $\theta(\eta)=\frac{T-T_H}{T_w-T_H}$, Using similarity transformation Equation (17) becomes:

$$\theta'' + (PrfR + \alpha\eta Pr)\theta' = 0 \tag{20}$$

$Pr = \frac{\rho C_p}{\kappa_\circ}$ is the Prandtl number. Boundary conditions for θ can be obtained from Equations

$$y = 0: \qquad \theta = 1 \tag{21}$$

$$y = 1: \qquad \theta = 0 \tag{22}$$

4. NUMERICAL COMPUTATION

In order to find the numerical solution, we employ shooting method to solve and investigate the multiple solutions of Equation (13-14) and (20) subject to the boundary conditions Equations (15-16) and (21-22).

For this we convert Equation (13-14) and (20) boundary value problem into initial value problem by setting:

$$\chi_1 = \eta, \chi_2 = f, \chi_3 = f', \chi_4 = f'', \chi_5 = f''', \chi_6 = g, \chi_7 = g', \chi_8 = \theta, \chi_9 = \theta'$$

$$\begin{pmatrix} \chi_1' \\ \chi_2' \\ \chi_3' \\ \chi_4' \\ \chi_5' \\ \chi_6' \\ \chi_7' \\ \chi_8' \\ \chi_9' \end{pmatrix} = \begin{pmatrix} 1 \\ \chi_3 \\ \chi_4 \\ \chi_5 \\ \frac{1}{(1+C_1)}\left(\frac{C_1}{\left(1+\frac{C_1}{2}\right)}\left(-N\alpha(3\chi_6 + \chi_1\chi_7) - NR(\chi_3\chi_6 - \chi_2\chi_7) + C_1(2\chi_6 - \chi_4)\right) - 3\alpha\chi_4 - \alpha\chi_1\chi_5 - R(\chi_3\chi_4 - \chi_2\chi_5)\right) \\ \chi_7 \\ \frac{C_1}{\left(1+\frac{C_1}{2}\right)}\left(-N\alpha(3\chi_6 + \chi_1\chi_7) - NR(\chi_3\chi_6 - \chi_2\chi_7) + C_1(2\chi_6 - \chi_4)\right) \\ \chi_9 \\ -(Pr\chi_2 + \alpha\chi_1 Pr)\chi_9 \end{pmatrix} \tag{23}$$

Subject to the initial conditions:

$$\begin{pmatrix} \chi_1 \\ \chi_2 \\ \chi_3 \\ \chi_4 \\ \chi_5 \\ \chi_6 \\ \chi_7 \\ \chi_8 \\ \chi_9 \end{pmatrix} = \begin{pmatrix} 1 \\ 1 \\ 0 \\ \beta \\ \gamma \\ 0 \\ \delta \\ 0 \\ \varepsilon \end{pmatrix} \tag{24}$$

Here, β, γ, δ and ε are unknown initial conditions. We have to shoot these initial conditions with some arbitrary slope such that solution of the system (23) satisfies the given conditions at the boundary. Hit and trail approach is acquire in order to find the unknown initial conditions. Once slope of β, γ, δ and ε assumed then numerical integration is made for the initial value problem and accuracy of missing initial conditions is then checked by comparing calculated value with the given terminal point. The details of shooting method with Maple implementation *shoot* has been described by Meade et al. [23].

5. RESULTS AND DISCUSSION

In this section, we study the effects of of Reynold number R, vortex viscosity parameter C_1, wall expansion ratio α and Prandtl number Pr on velocity $f'(\eta)$, micro-rotation $g(\eta)$ and temperature profile $\theta(\eta)$. Moreover, effect of these parameters on shear and couple stresses is also discussed in the form of tabulation representation. For this purpose we have prepared tables and figures to demonstrate the effects of these parameters briefly.

Table 1: Effects of Reynold number R, vortex viscosity parameter C_1 and wall expansion ratio α on shear and couple stress at the wall

R	C_1	α	I-Type Solution		II-Type Solution		III-Type Solution	
			$f''(1)$	$g'(1)$	$f''(1)$	$g'(1)$	$f''(1)$	$g'(1)$
40	0.3	-0.5	-8.005579	0.155951	-15.69354	1.582672	-32.220054	0.643720
		-0.3	-7.647417	0.240592	-14.191112	1.389367	-31.348314	0.643122
		-0.1	-7.133580	0.449830	-12.73455	1.111721	-30.48721	0.642870
		0.1	-6.328660	1.048944	-11.42021	0.787151	-29.63664	0.642993
		0.3	-5.034100	2.770737	-10.37298	0.505138	-28.79648	0.643519
		0.5	-3.105862	6.145867	-9.637289	0.324069	-27.96660	0.644481
40	0.1	0.1	-6.328660	1.048944	-11.420211	0.7871513	-29.636649	0.642993
	0.3		-4.879977	1.812693	-12.232172	2.203667	-27.101721	1.653356
	0.5		-3.916973	2.181498	-14.242791	2.998649	-24.352902	2.439703
30	0.1	0.1	-4.116602	0.668627	-13.84659	0.638262	-24.936474	0.537415
40			-6.328660	1.048944	-11.420211	0.7871513	-29.636649	0.642993
50			-8.809910	1.556109	-11.860050	0.7912084	-33.437599	0.791893

Table 1 presented the effects of Reynold number R, vortex viscosity parameter C_1 and wall expansion ratioα on shear and couple stress at the wall. It can be seen from these numerical representation that magnitude of the shear stress decreases gradually by the increasing values of wall expansion ratio $\alpha \in [-0.5,0.5]$. Physically we can say that fluid velocity increases due to decreasing trend of wall drag, it only because of the fact that wall expansion $\alpha \geq -0.5$ decrease the boundary layer thickness and allows the fluid to move in a channel freely which causes the increase in the velocity. Effects of Reynold number R and vortex viscosity parameter C_1 on shear and couple stress is also discussed in this table only for the expanding wall $\alpha > 0$. Furthermore, numerical values of the skin friction at the wall $f''(1)$ increases which causes the falloff the

velocity of the fluid near the channel wall for I and III-Type of solution. This result is a good argument of the previously published experimental work of Hayt & Fabula [24] in 1964. They claimed that non-Newtonian fluids offered great reduction in the velocity of the fluid near the rigid body. So without loss of any generality we can say that our obtained numerical results are up to the mark and having a great argument of the previously published worked. Table 2 presented the numerical values of heat transfer rate at the walls for the various values of Prandtl number. From this presentation of numerical values of heat transfer it can be argued that numerical values of heat transfer lean towards decreasing in nature by the increasing values of Prantdl number for all the branches of the solutions. In Figure 2, we have plotted the values of skin friction $f''(1)$ against the values of wall expansion ratio α for the fixed values of $R = 40, C_1 = 0.3$ and $N = 1$. It is noticed that the value of skin friction $f''(1)$ increasing monotonically for all solutions. This means that increase in the wall expansion ratio $\alpha > 0$ provided the space to the fluid to flow easily in a channel however totally opposite behavior is observed for wall contraction case $\alpha < 0$. In Figure 3 we correlate the effect of Reynold number R on heat transfer at the channel wall. It is depicted that I and II-Type of solutions behave asymptotic to the horizontal axis $y = 0$ as the increase values of suction. We can say that heat transfer $|\theta'(1)|$ decreases and tends to zero as the increasing values of Reynold number. However, for III-Type of solution heat transfer increases initially but gradually decreases. As indicated by Mishra and DebRoy [25], multiple solutions exist for many complex fluid flow problems in fluid dynamics and heat transfer because of highly nonlinear problems. It is worthy to compute the unstable states as well as stable ones, since solution emerging from bifurcations along unstable solutions often connect with stable solution delivering generally mystifying phenomena ([26]). The transition process provides valuable information regarding flow evolution and can be used to confirm flow stability. The transition to multiplicity of solutions takes place below any threshold to chaos or turbulence. In heat transfer engineering, the flow multiplicity and instability may strongly influence the quality and structure of the final product in material processing ([25]) as example and better insight about the development of stability and multiplicity of flow states can serve to stimulate innovations as well as may lead to improvements in the performance, reliability and costs of many practical flow problems such as crystal growth processes, rotating machines ([27]). We notice also the fact that Ma and Hui [28] have shown that for some special cases of the two-dimensional unsteady boundary-layer equations, five different solutions of the governing equations exist.

Table 2: Effect of Prandtl number Pr on $\theta'(1)$

Pr	I-Type Solution	II-Type Solution	III-Type Solution
	$\theta'(1)$	$\theta'(1)$	$\theta'(1)$
0.5	-0.010247437	-0.019265008	-0.51147143
1.5	-2.47E-07	-2.14E-06	-0.0336541
2.5	-4.44E-12	-1.80E-10	-0.00302957

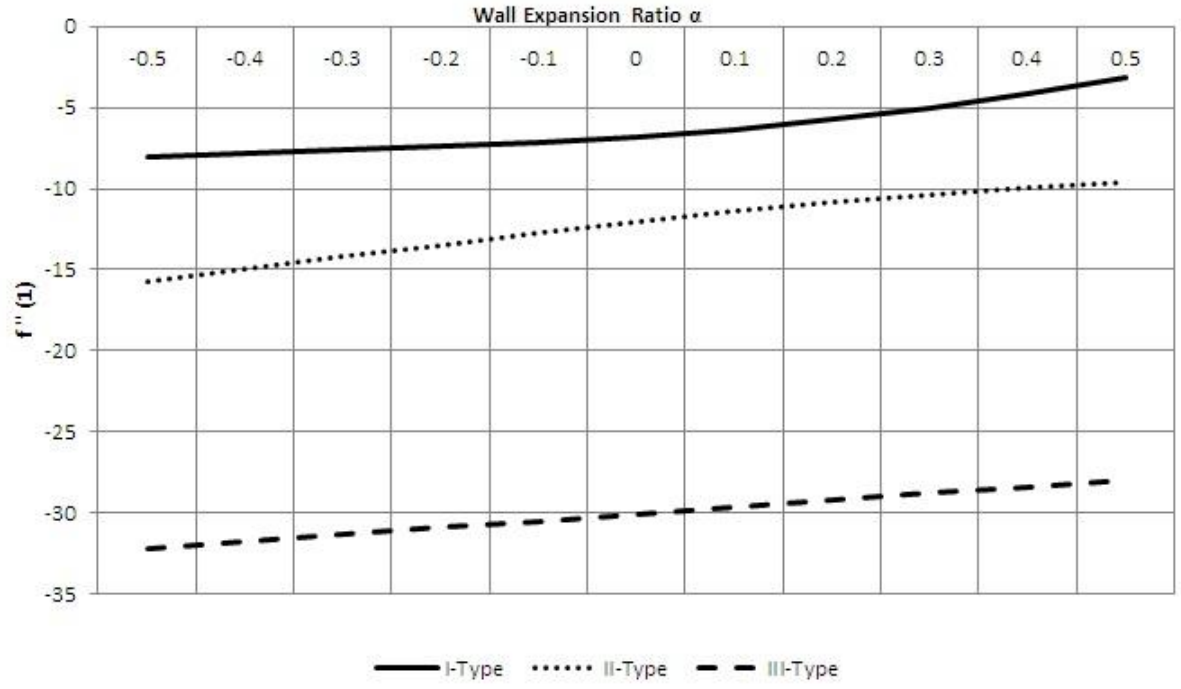

Figure 2: Skin friction against the values of wall expansion ratio

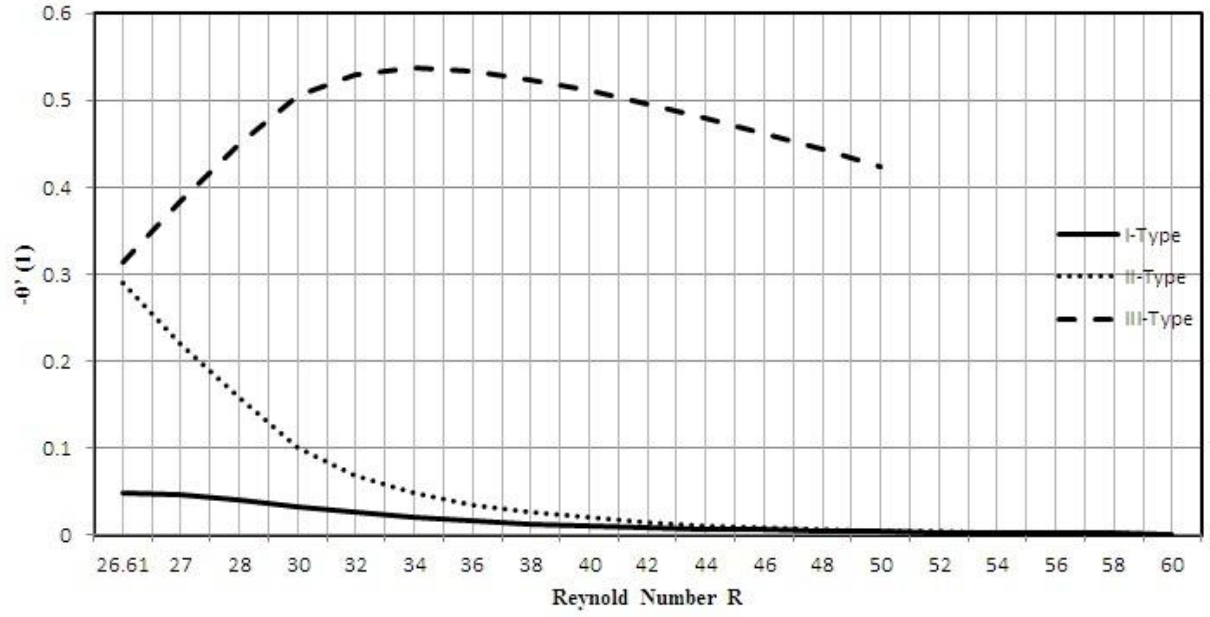

Figure 3: Heat transfer $|\theta'(1)|$ against the values of Reynold number R

Figure 4 and 5 presented the effects of wall expansion $\alpha > 0$ on velocity profile $f'(\eta)$ and micro-rotation $g(\eta)$ respectively for $C_1 = 0.3, R = 40$ and $N = 1$. Velocity of the fluid particles

near the channel walls decreases as the increase values of wall expansion $\alpha > 0$ for all the multiple solutions. Profile of the micro-rotation $g(\eta)$ is increasing by the enhancement of the $\alpha > 0$ for I and II-Type of the solutions. However, for the III-Type of solution profile is twisted into two phase and can be seen clearly in Figure 5. Furthermore, effect of wall contraction $\alpha < 0$ on velocity profile $f'(\eta)$ is shown in Figure 6 and observed that the effect of wall contraction $\alpha < 0$ on velocity profile $f'(\eta)$ is opposite to the effect of wall expansion $\alpha > 0$. Micro-rotation $g(\eta)$ increases by increasing the numerical values of wall contraction $\alpha < 0$ for the I-Type of solution and decreases for the II and III-Type of solutions.

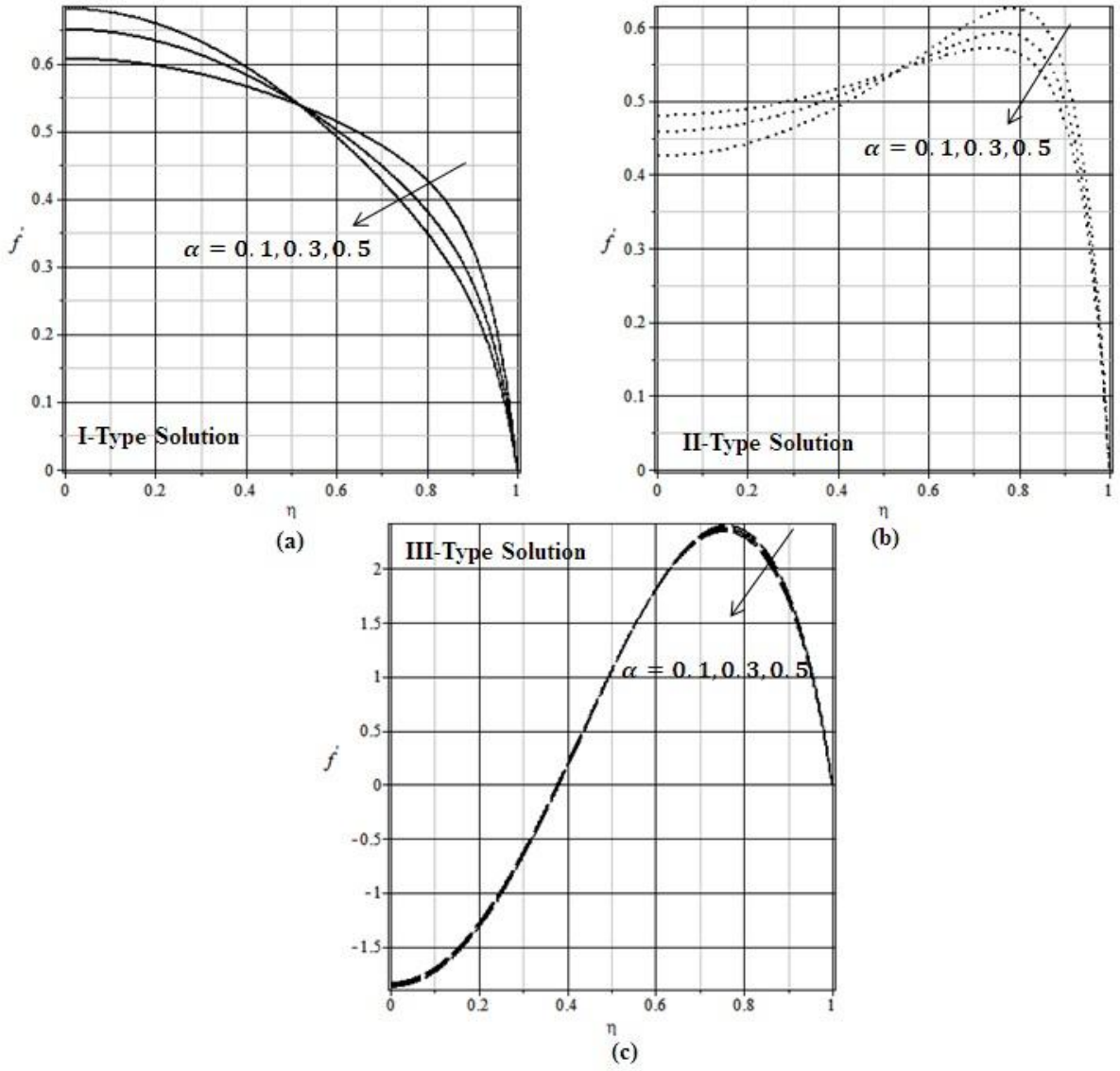

Figure 4: Effect of wall expansion $\alpha > 0$ on velocity profile $f'(\eta)$ for $C_1 = 0.3, R = 40$ and $N = 1$

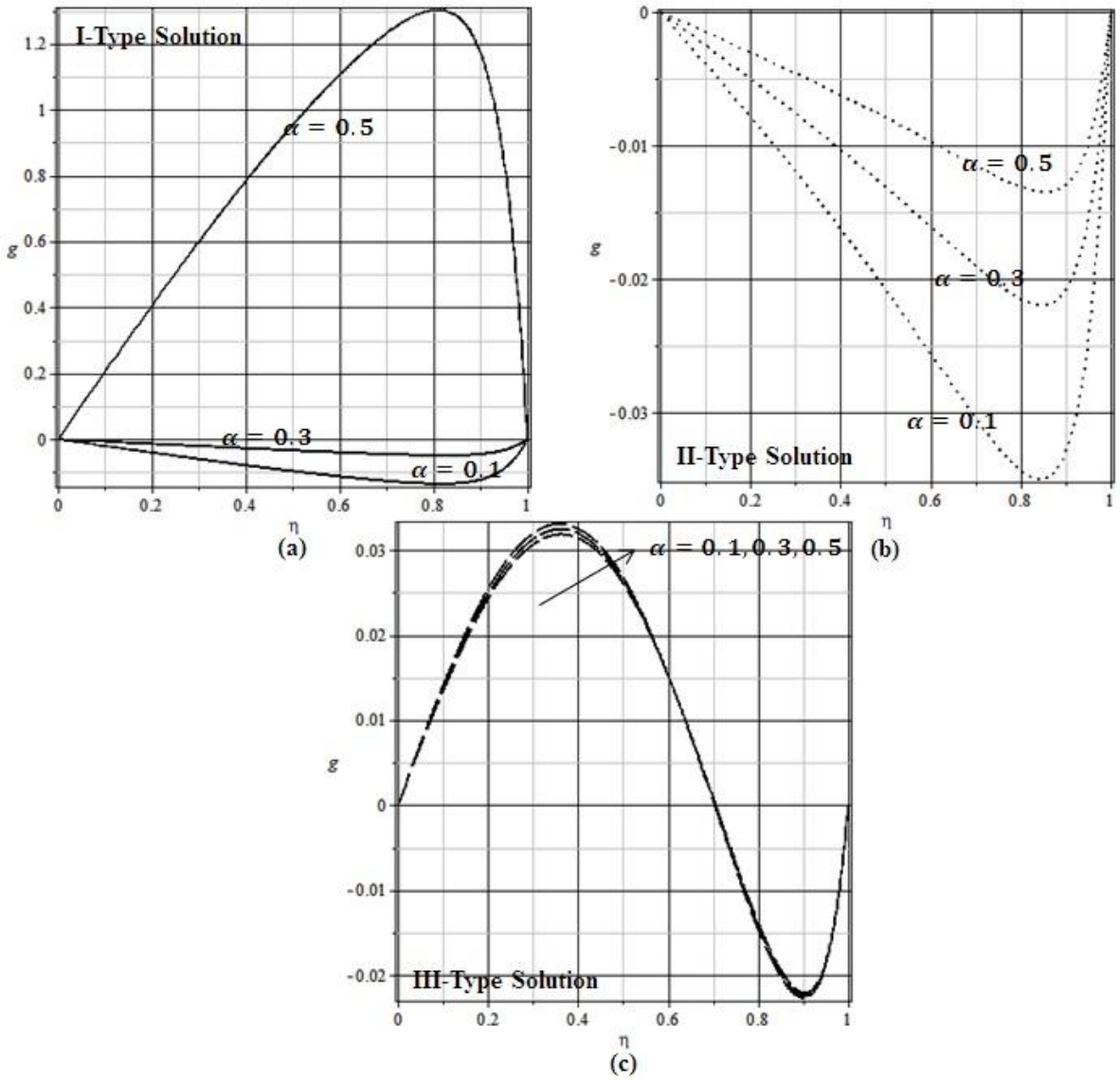

Figure 5: Effect of wall expansion $\alpha > 0$ on micro-rotation $g(\eta)$for $C_1 = 0.3, R = 40$ and $N = 1$

Effect of C_1 on velocity profile $f'(\eta)$ for $\alpha = 0.3, R = 40$ and $N = 1$ is identified in Figure 8. It is founded that velocity of the fluids decreases near the channel wall for the I and III-Type of solutions by increasing the values of C_1. It is due to the fact that micropolar fluids offer great resistance near the rigid body. However, totally opposite trend is seen for the II-Type of solution. Effect of C_1 on micro-rotation $g(\eta)$ for $\alpha = 0.3, R = 40$ and $N = 1$ is viewed in Figure 9. Figure 10 illustrated the effects of Reynold number R on velocity profile $f'(\eta)$ for $\alpha = 0.3, C_1 = 0.3$ and $N = 1$. From this Figure it can be viewed that velocity of the fluid increases near the channel wall by increasing the numerical values of Reynold number for I and III-Type of solutions and opposite effect can be seen for II-Type of solution. Effect of Reynold number R on micro-rotation $g(\eta)$ for $\alpha = 0.3, C_1 = 0.3$ and $N = 1$ is depicted from Figure 11. Micro-rotation profile squeeze done for I and II-Type of solutions and increasing in nature for the III-Type of

solution. Figure 12 reflected the effect of Prandtl number Pr on Temperature profile $\theta(\eta)$. An increase in the strength of Prandtl number reduces the temperature profile $\theta(\eta)$ for I and II-Type of solutions. For the III-type of solution temperature profile $\theta(\eta)$ decrease near the channel wall $\eta \approx 1$ and increases rest of the channel.

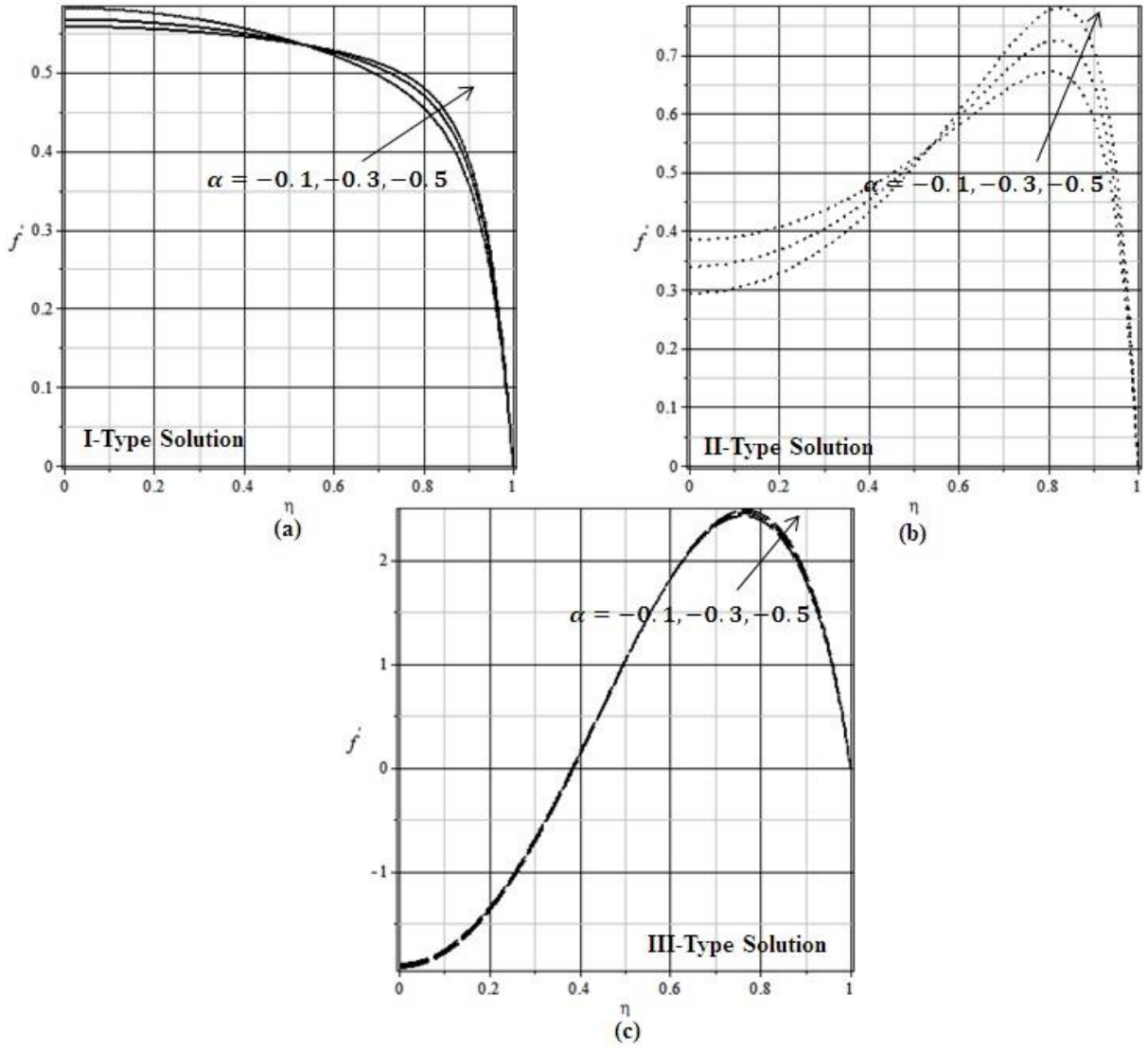

Figure 6: Effect of wall contraction $\alpha < 0$ on velocity profile $f'(\eta)$ for $C_1 = 0.3, R = 40$ and $N = 1$

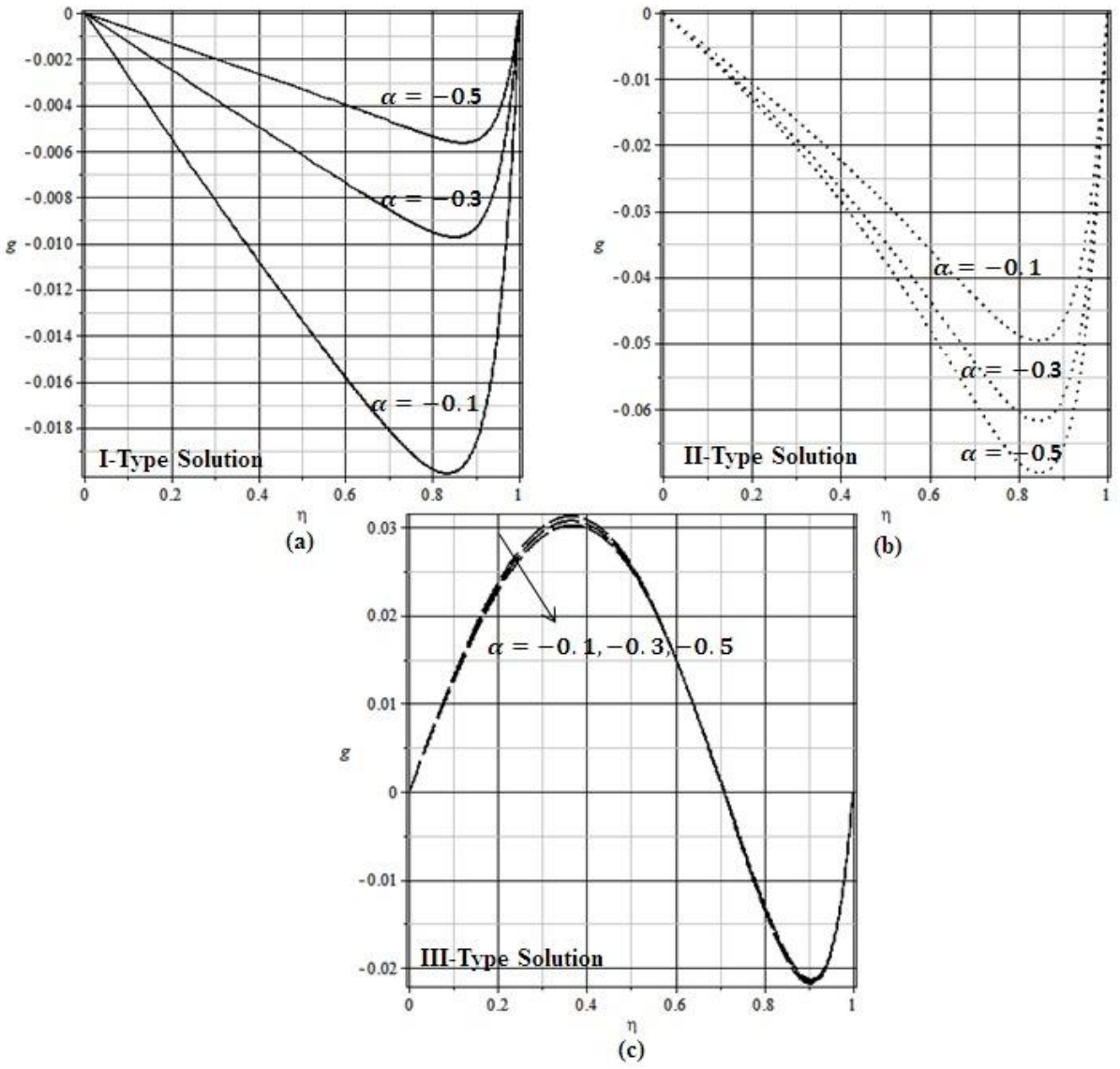

Figure 7: Effect of wall expansion $\alpha < 0$ on micro-rotation $g(\eta)$ profile $f'(\eta)$ for $C_1 = 0.3, R = 40$ and $N = 1$

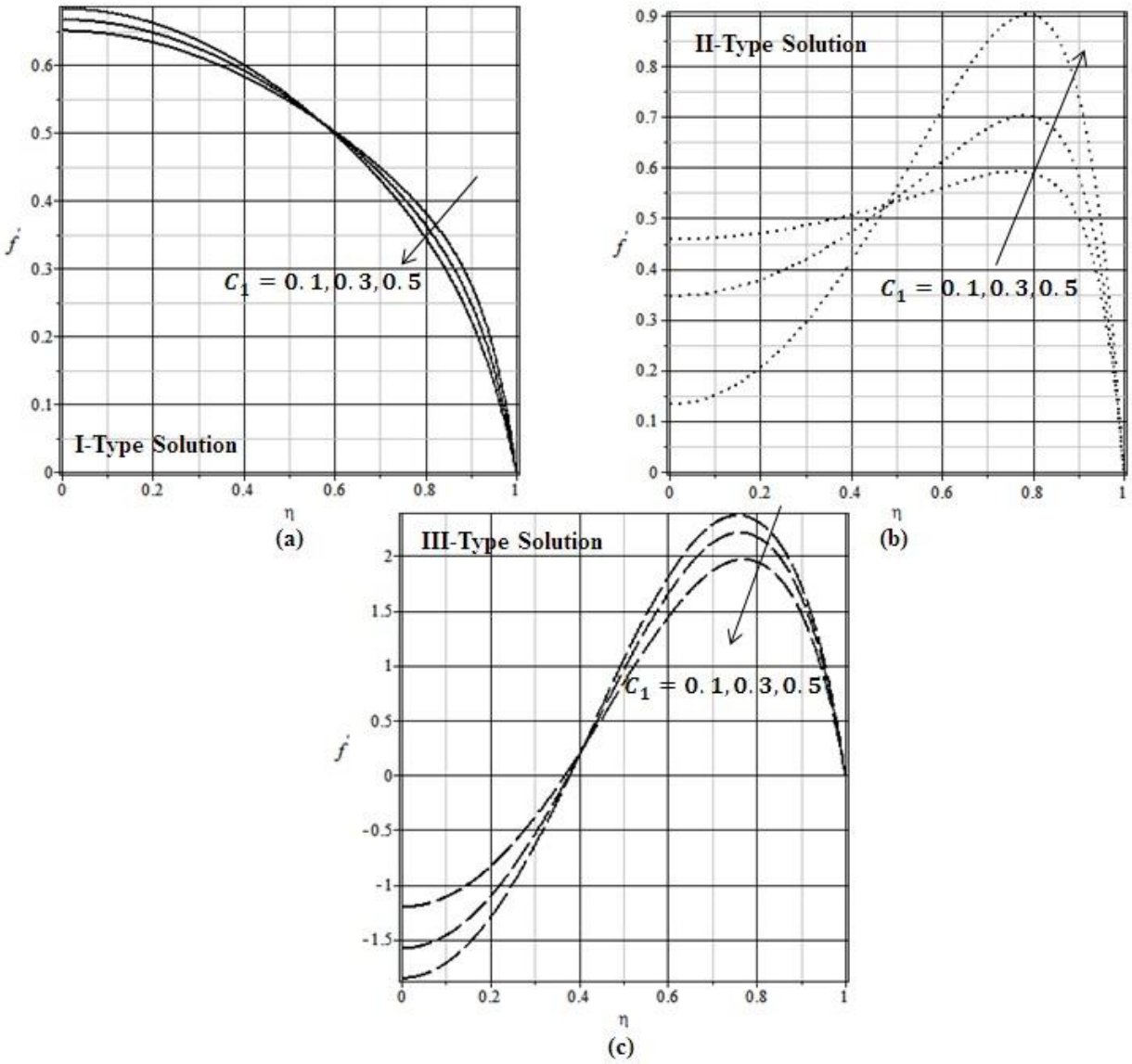

Figure 8: Effect of C_1on velocity profile $f'(\eta)$ for $\alpha = 0.3, R = 40$ and $N = 1$

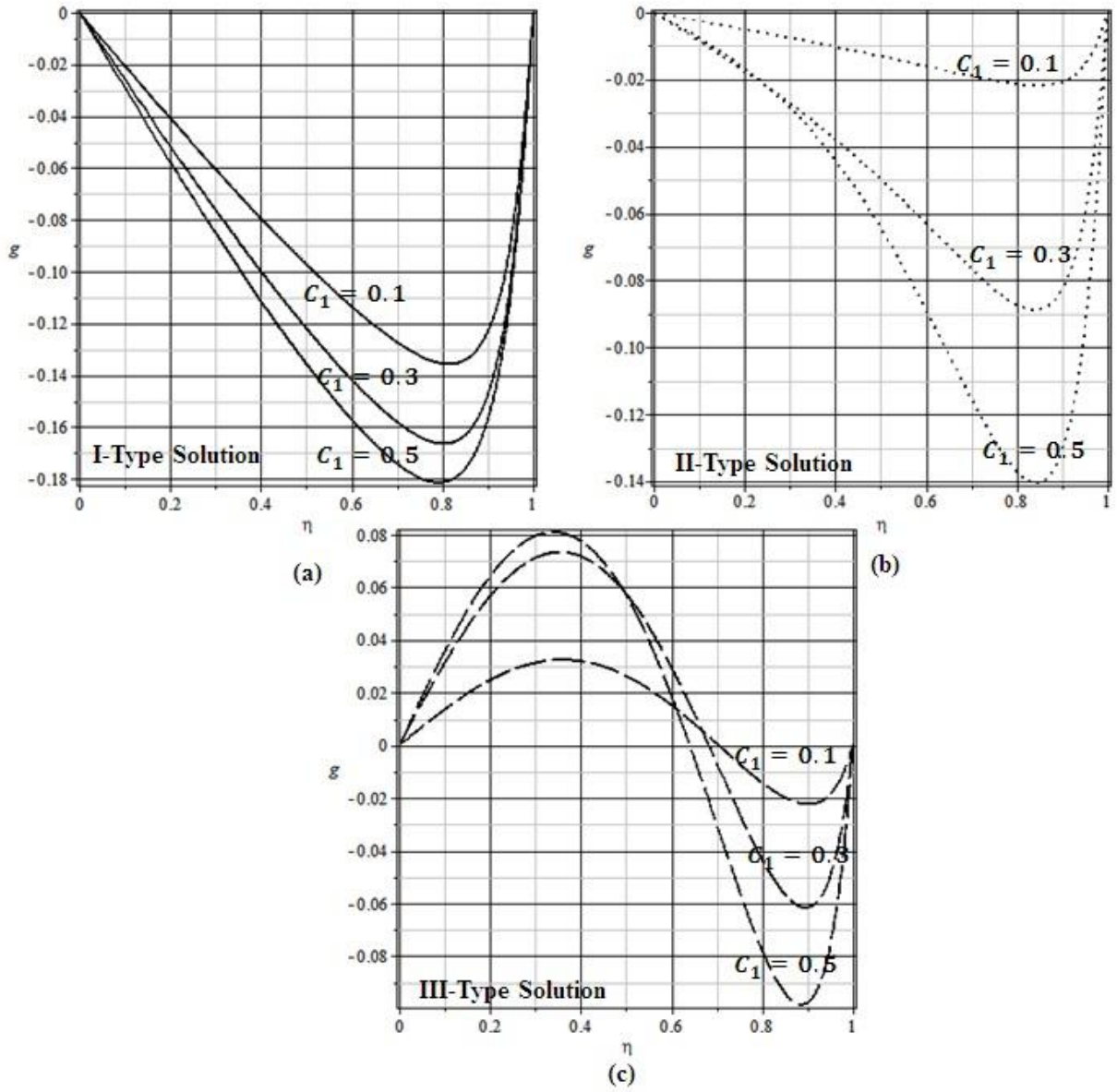

Figure 9: Effect of C_1 on micro-rotation $g(\eta)$ for $\alpha = 0.3, R = 40$ and $N = 1$

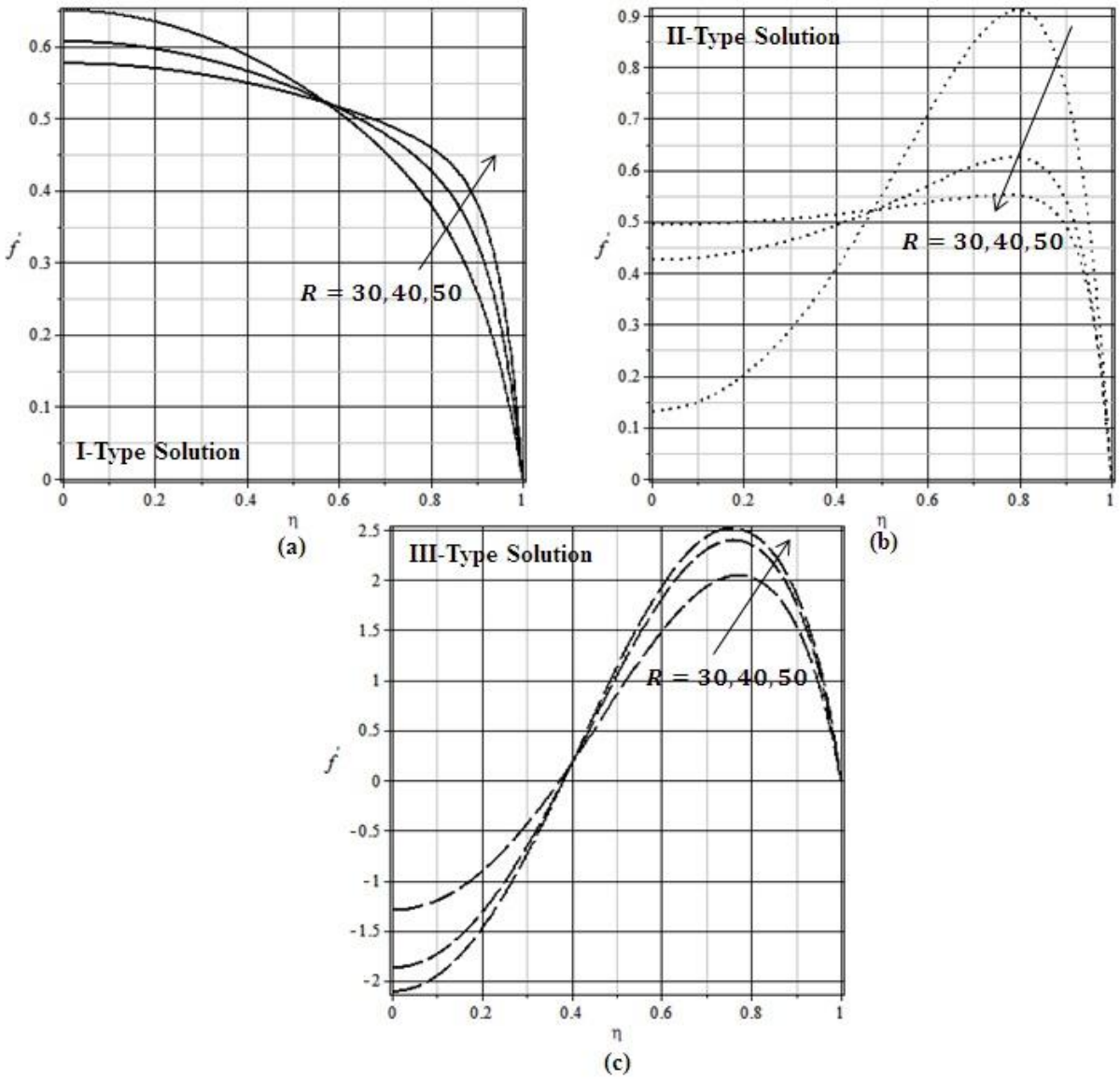

Figure 10: Effect of Reynold number R on velocity profile $f'(\eta)$ for $\alpha = 0.3, C_1 = 0.3$ and $N = 1$

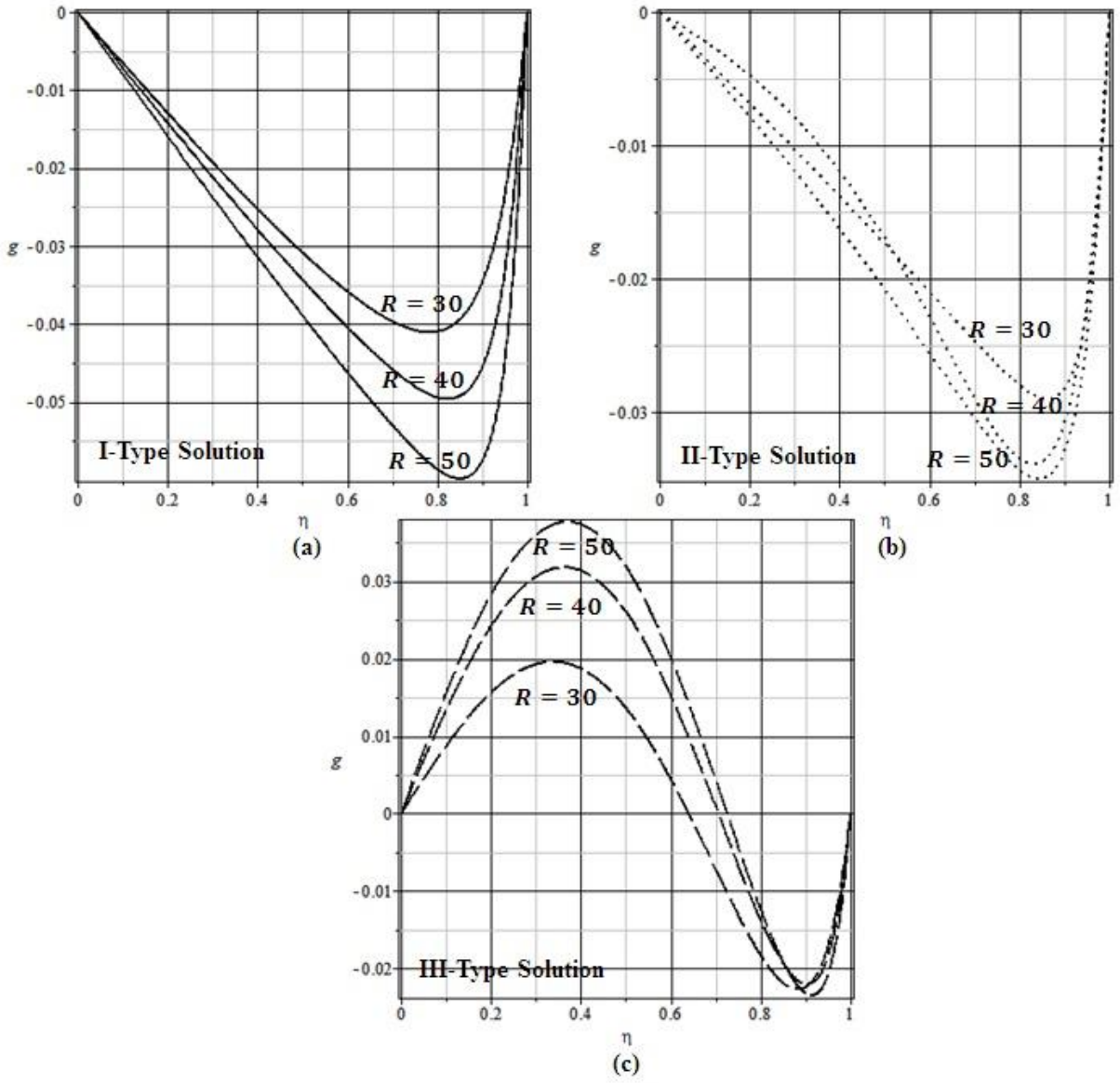

Figure 11: Effect of Reynold number R on micro-rotation $g(\eta)$ for $\alpha = 0.3, C_1 = 0.3$ and $N = 1$

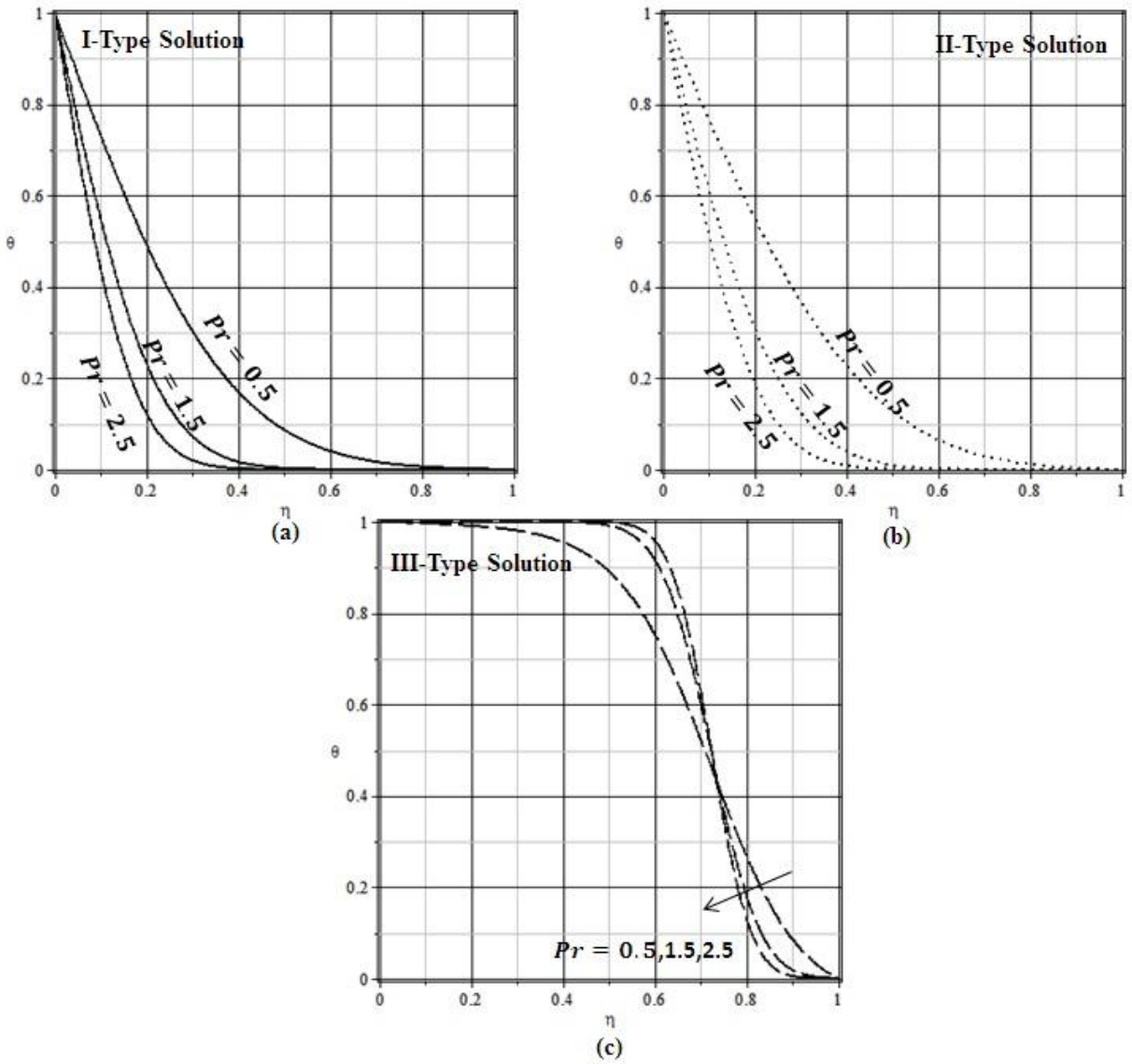

Figure 12: Effect of Prandtl number Pr on Temperature profile $\theta(\eta)$

REFERENCES

[1] Ali, K. and Ashraf, M., 2014. Numerical simulation of the micropolar fluid flow and heat transfer in a channel with a shrinking and a stationary wall.Journal of Theoretical and Applied Mechanics, 52.

[2] Majdalani, J., 2008. Exact Navier-Stokes Solution for the Pulsatory Viscous Channel Flow with Arbitrary Pressure Gradient. Journal of Propulsion and Power, 24(6), pp.1412-1423.

[3] Rawool, A.S., Mitra, S.K. and Kandlikar, S.G., 2006. Numerical simulation of flow through microchannels with designed roughness. Microfluidics and nanofluidics, 2(3), pp.215-221.

[4] Dehghan, M., Jamal-Abad, M.T. and Rashidi, S., 2014. Analytical interpretation of the local thermal non-equilibrium condition of porous media imbedded in tube heat exchangers. Energy Conversion and Management,85, pp.264-271.

[5] A. Rauf, S. A. Shahzad, M. K. Siddiq, J. Raza, and M. A. Meraj, 2016. Mixed convective thermally radiative micro nanofluid flow in a stretchable channel with porous medium and magnetic field. AIP Advances 6, 035126 (2016); doi: 10.1063/1.4945369

[6] A. C. Eringen, Theory of micropolar fluids, J. Math. Mech, 16 (1966) 1-18.

[7] Mekheimer, K.S. and El Kot, M.A., 2008. The micropolar fluid model for blood flow through a tapered artery with a stenosis. Acta Mechanica Sinica,24(6), pp.637-644.

[8] Nadeem, S., Akbar, N.S. and Malik, M.Y., 2010. Exact and numerical solutions of a micropolar fluid in a vertical annulus. Numerical Methods for Partial Differential Equations, 26(6), pp.1660-1674.

[9] Hudimoto, B. and Tokuoka, T., 1969. 2-DIMENSIONAL SHEAR FLOWS OF LINEAR MICROPOLAR FLUIDS. International Journal of Engineering Science, 7(5), p.515.

[10] Lockwood, F.E., Benchaita, M.T. and Friberg, S.E., 1986. Study of lyotropic liquid crystals in viscometric flow and elastohydrodynamic contact. ASLE transactions, 30(4), pp.539-548.

[11] Ariman, T.T.N.D., Turk, M.A. and Sylvester, N.D., 1974. Applications of microcontinuum fluid mechanics. International Journal of Engineering Science, 12(4), pp.273-293.

[12] Gorla, R.S.R., Pender, R. and Eppich, J., 1983. Heat transfer in micropolar boundary layer flow over a flat plate. International Journal of Engineering Science, 21(7), pp.791-798.

[13] Rees, D.A.S. and Basson, A.P., 1996. The Blasius boundary-layer flow of a micropolar fluid. International Journal of Engineering Science, 34(1), pp.113-124.

[14] Kelson, N.A. and Desseaux, A., 2001. Effect of surface conditions on flow of a micropolar fluid driven by a porous stretching sheet. International journal of engineering science, 39(16), pp.1881-1897.

[15] Joneidi, A.A., Ganji, D.D. and Babaelahi, M., 2009. Micropolar flow in a porous channel with high mass transfer. International Communications in Heat and Mass Transfer, 36(10), pp.1082-1088.

[16] Aski, F.S., Nasirkhani, S.J., Mohammadian, E. and Asgari, A., 2014. Application of Adomian decomposition method for micropolar flow in a porous channel. Propulsion and Power Research, 3(1), pp.15-21.

[17] Sheikholeslami, M., Hatami, M. and Ganji, D.D., 2014. Micropolar fluid flow and heat transfer in a permeable channel using analytical method. Journal of Molecular Liquids, 194, pp.30-36.

[18] Sajid, M., Abbas, Z. and Hayat, T., 2009. Homotopy analysis for boundary layer flow of a micropolar fluid through a porous channel. Applied Mathematical Modelling, 33(11), pp.4120-4125.

[19] Fakour, M., Vahabzadeh, A., Ganji, D.D. and Hatami, M., 2015. Analytical study of micropolar fluid flow and heat transfer in a channel with permeable walls. Journal of Molecular Liquids, 204, pp.198-204.

[20] Mehmood, R., Nadeem, S. and Masood, S., 2016. Effects of transverse magnetic field on a rotating micropolar fluid between parallel plates with heat transfer. Journal of Magnetism and Magnetic Materials, 401, pp.1006-1014.

[21] S. Uchida, H. Aoki, Unsteady flows in a semi-infinite contracting or expanding pipe, *J. Fluid Mech.* **82**, 371–387, 1977.
[22] C.E. Dauenhauer, J. Majdalani, Exact self-similarity solution of the Navier–Stokes equations for a porous channel with orthogonally moving walls, *Phys. Fluids* **15**,1485–1495, 2003.
[23] Meade, D.B., Haran, B.S. and White, R.E., 1996. The shooting technique for the solution of two-point boundary value problems. Maple Technical Newsletter, 3(1).
[24] Hoyt, J.W. and Fabula, A.G., 1964. THE EFFECT OF ADDITIVES ON FLUID FRICTION (No. NOTS-TP-3670). NAVAL ORDNANCE TEST STATION CHINA LAKE CALIF. New York, 2003.
[25] Mishra, S. and DebRoy, T., 2005. A computational procedure for finding multiple solutions of convective heat transfer equations. Journal of Physics D: Applied Physics, 38(16), p.2977.
[26] Cliffe, K.A., Spence, A. and Tavener, S.J., 2000. The numerical analysis of bifurcation problems with application to fluid mechanics. Acta Numerica 2000, 9, pp.39-131.
[27] Gelfgat, A.Y. and Bar-Yoseph, P.Z., 2004. Multiple solutions and stability of confined convective and swirling flows-a continuing challenge. International Journal of Numerical Methods for Heat & Fluid Flow, 14(2), pp.213-241.
[28] Ma, P.K. and Hui, W.H., 1990. Similarity solutions of the two-dimensional unsteady boundary-layer equations. Journal of Fluid Mechanics, 216, pp.537-559.

HIGHLIGHTS

- Heat transfer analysis of micropolar fluid in a channel with changing walls is considered.
- Mathematical modeling for the law of conservation of mass, momentum, angular momentum and energy profiles is performed.
- New branches of the solution for the variation of different physical parameters are investigated.
- Triple solutions of micropolar fluid in a channel with changing walls occurred only for the case of suction such that $R \geq 26.61$.
- Velocity profile increases near the center of the channel as $\alpha > 0$ and decreases as $\alpha < 0$.